Supporting information

Anisotropic 2D $Cu_{2-x}Se$ Nanocrystals from Dodecaneselenol and their Conversion to CdSe and $CuInSe_2$ Nanoparticles

Anne C. Berends[†], Ward van der Stam[†], Quinten A. Akkerman[†], Johannes D. Meeldijk[‡], Joost van der Lit[†], and Celso de Mello Donega[†]*

† Condensed Matter and Interfaces, Debye Institute for Nanomaterials Science, Utrecht University, P.O. Box 80000, 3508 TA Utrecht, The Netherlands.

‡ Electron Microscopy Utrecht, Debye Institute for Nanomaterials Science, Utrecht University, 3584 CH Utrecht, Netherlands.

***Corresponding Author**: email: c.demello-donega@uu.nl

Assignment of the peaks observed in the ^{1}H-NMR spectrum of the product of the DDSe synthesis (Figure 1 in the main text).

The majority of the peaks observed in the ^{1}H-NMR spectrum can be assigned to the desired product 1-dodecaneselenol (DDSe).[1,2] The triplet at 0.85 ppm is assigned to the $–CH_3$ protons at the end of the alkyl chain of DDSe. The $-CH_2-$ protons next to the –SeH group shift to 2.58 ppm, compared to 1.25 ppm for the $-CH_2-$ protons in the middle of the alkyl chain. The quintet at 1.75 ppm is ascribed to the $–CH_2-$ protons next to the $–CH_2SeH$ group, as these protons still feel the electronegative selenium atom. Finally, the selenol proton gives rise to a triplet at -0.7 ppm. Some of the observed peaks are assigned to impurities: the weak peaks at 3.62 and 2.79 ppm are assigned to protons that are part of a diselenide group (DDSe-DDSe), as two electronegative selenium atoms next to each other will give rise to larger chemical shifts. Another impurity present is a protonated alkyl chain, dodecane (DDH), which leads to proton signals overlapping with the broad peak at 1.5-1.2 ppm. The purity of the product dodecaneselenol can thus be calculated by comparing the peaks at 1.5-1.2 ppm (DDSe + DDSe-SeDD + DDH), the peak at 2.58 ppm (DDSe + DDSe-SeDD) and the peak at 3.62 ppm (DDSe-SeDD), which indicates that the product consists of 76% DDSe, 22% DDH and 2% DDSe-SeDD.

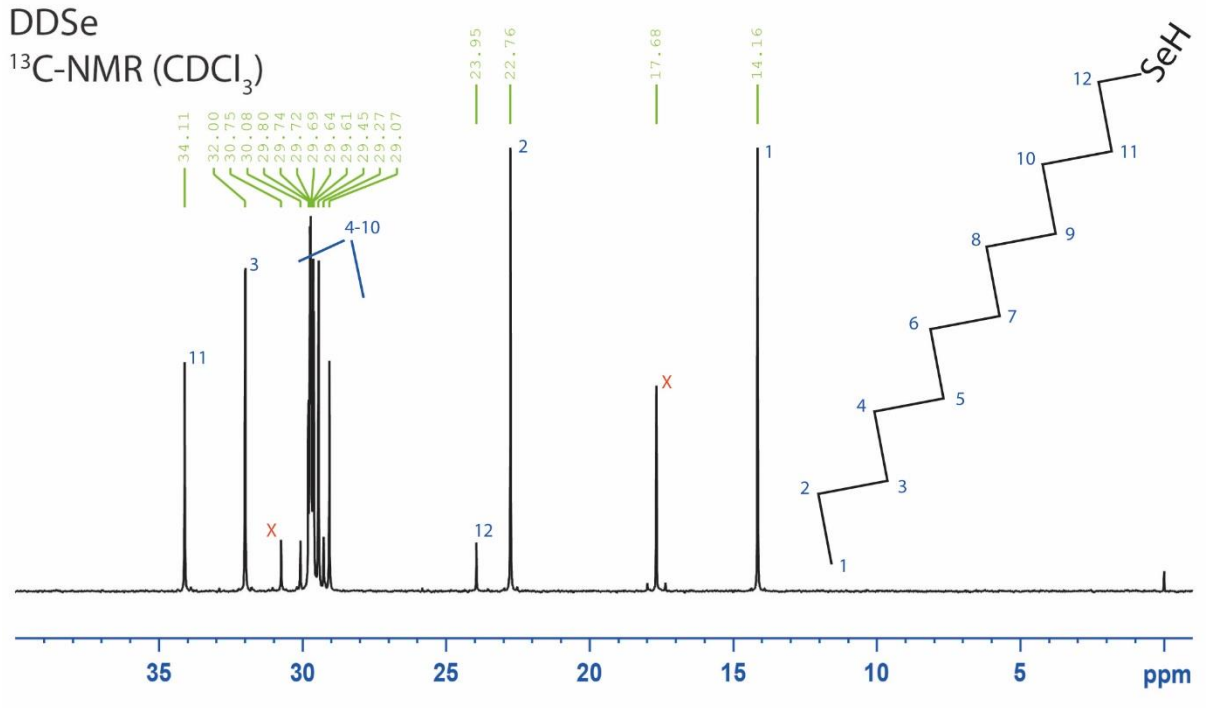

Figure S1. ^{13}C-NMR spectrum of DDSe product mixture. The blue numbers in the spectrum indicate the carbon atoms that the peaks are assigned to. The red crosses indicate peaks assigned to by-products of the synthesis.

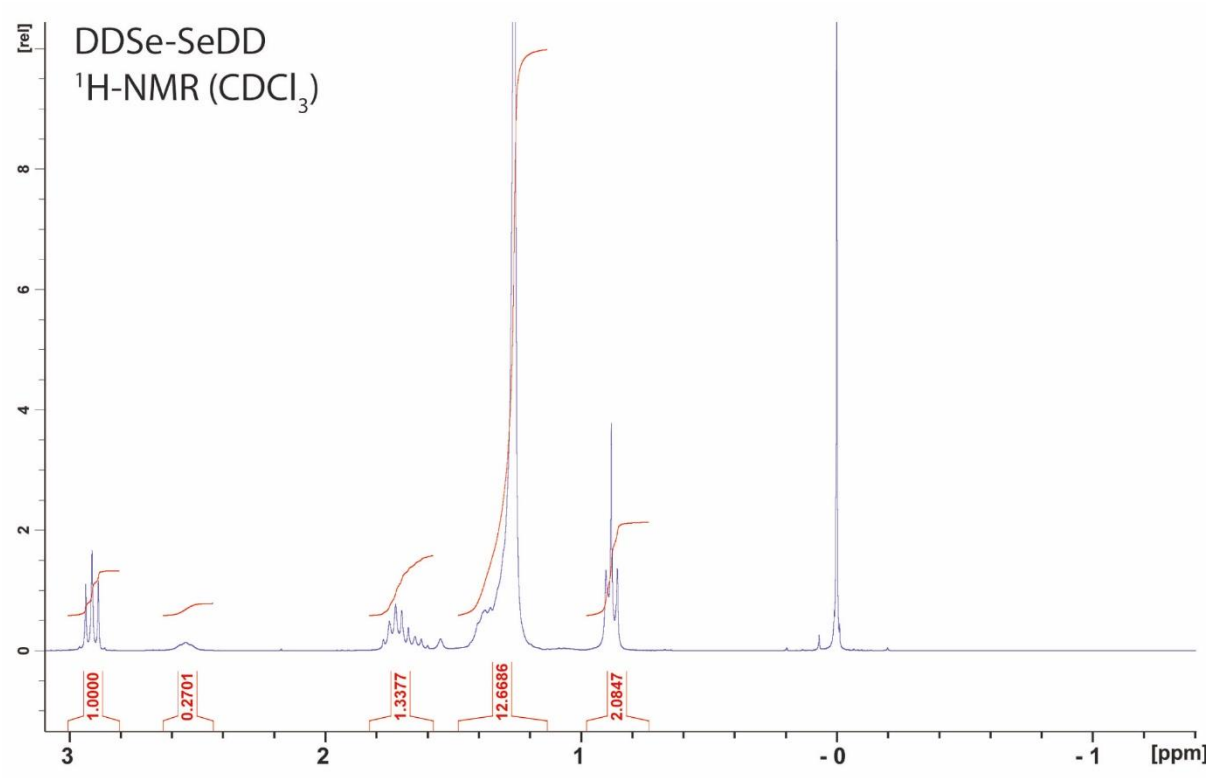

Figure S2. ^{1}H-NMR spectrum of yellow crystals isolated after a week exposure to light and air, showing formation of DDSe-SeDD with a purity of 96%.

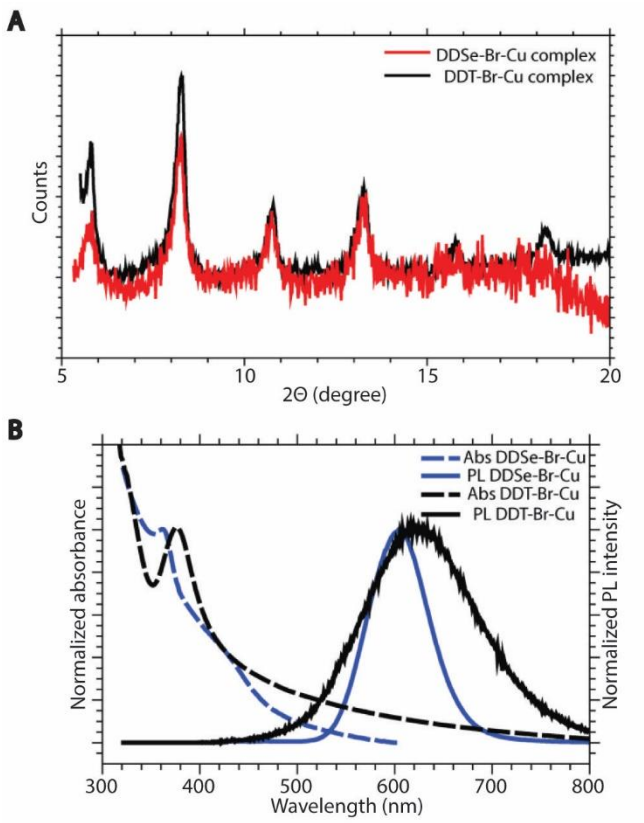

Figure S3. A. X-ray powder diffractogram of a sample taken 1 minute after injection of DDSe in a $Cu_{2-x}Se$ NCs synthesis (red) or DDT in a $Cu_{2-x}S$ NCs synthesis (black). **B**. Absorption (dashed lines) and PL (solid lines) spectra of samples taken 1 minute after injection of DDSe (blue) and DDT (black). The Cu-Br-DDSe optical spectra are ~15 nm blue-shifted compared to the Cu-Br-DDT spectra, and the DDSe PL spectrum is much narrower and appears much brighter than that observed for the S-analogue. Optical transitions in Cu(I) complexes are ascribed to ligand-to-metal-charge-transfer (LMCT) transitions[3] that shift to shorter wavelengths with decreasing electronegativity of the ligand. The blue-shift observed here for the Se-complexes with respect to the S-analogues is therefore explained by the replacement of S by the less electronegative Se. The PL quantum yield (QY) of a LMCT transition is determined by the balance between the radiative and non-radiative decay rates, the former being dictated by selection rules. For both complexes the transition is spin-forbidden, however the spin-selection rule is relaxed when heavier elements are involved, due to spin-orbit coupling.[4] The transition involving the heavier element selenium is therefore more efficient, since it has a faster radiative decay rate, which makes it more competitive with respect to the non-radiative decay processes. The band width of LMCT transitions is determined by the magnitude of the nuclear reorganization of the complex due the creation of an electron-hole pair.[4] As the soft Lewis acid Cu^+ binds stronger to the softer base selenium compared to sulfur, the creation of an exciton leads to a smaller degree of reorganization and consequently a narrower PL band.

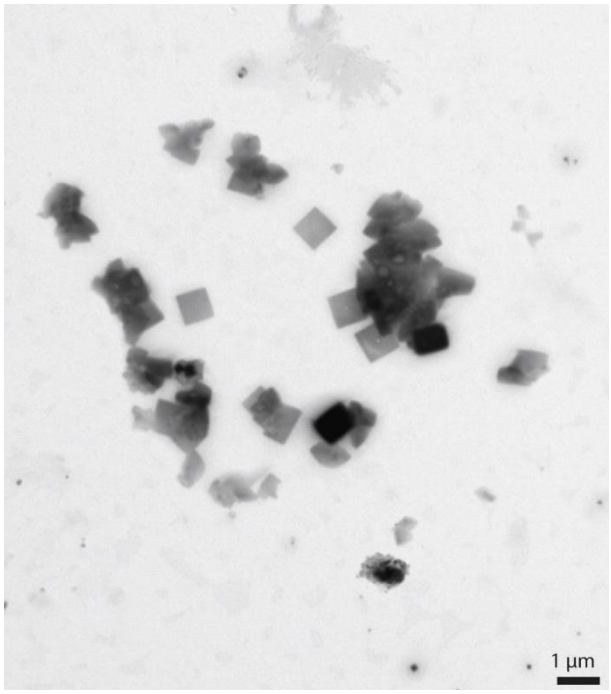

Figure S4. TEM image of product material one minute after injection of DDSe into the reaction mixture (0.22 mmol Cu(OAc), 0.075 mmol $SnBr_4.H_2O$, 12.5 mL ODE and 0.55 g TOPO) at 220 °C.

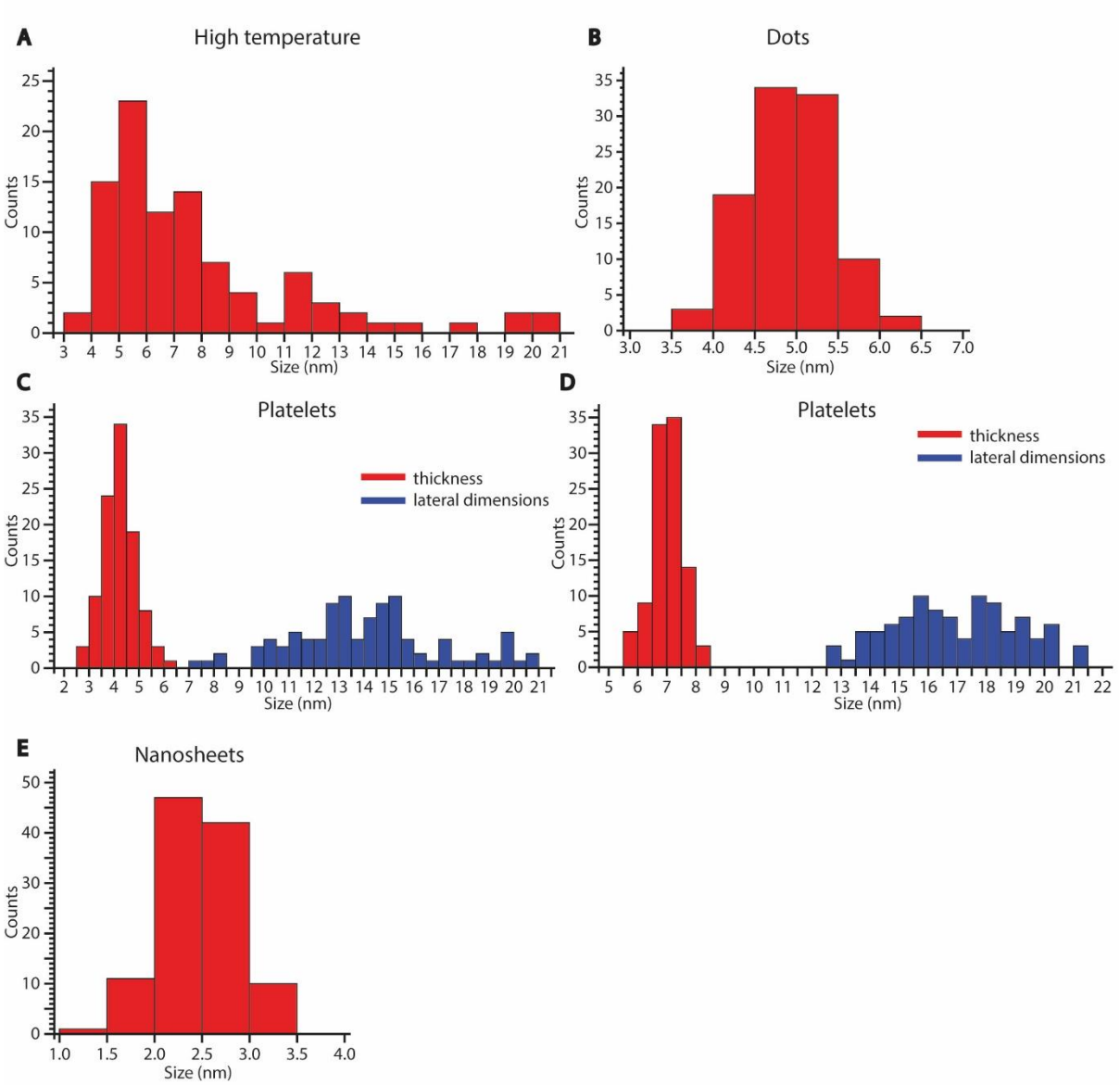

Figure S5. Size histograms of colloidal $Cu_{2-x}Se$ NCs shown in Figure 2 of the main text. **A.** Sample obtained at a reaction temperature of 220 °C. **B-E** Samples obtained in different syntheses at a reaction temperature of 170 °C.

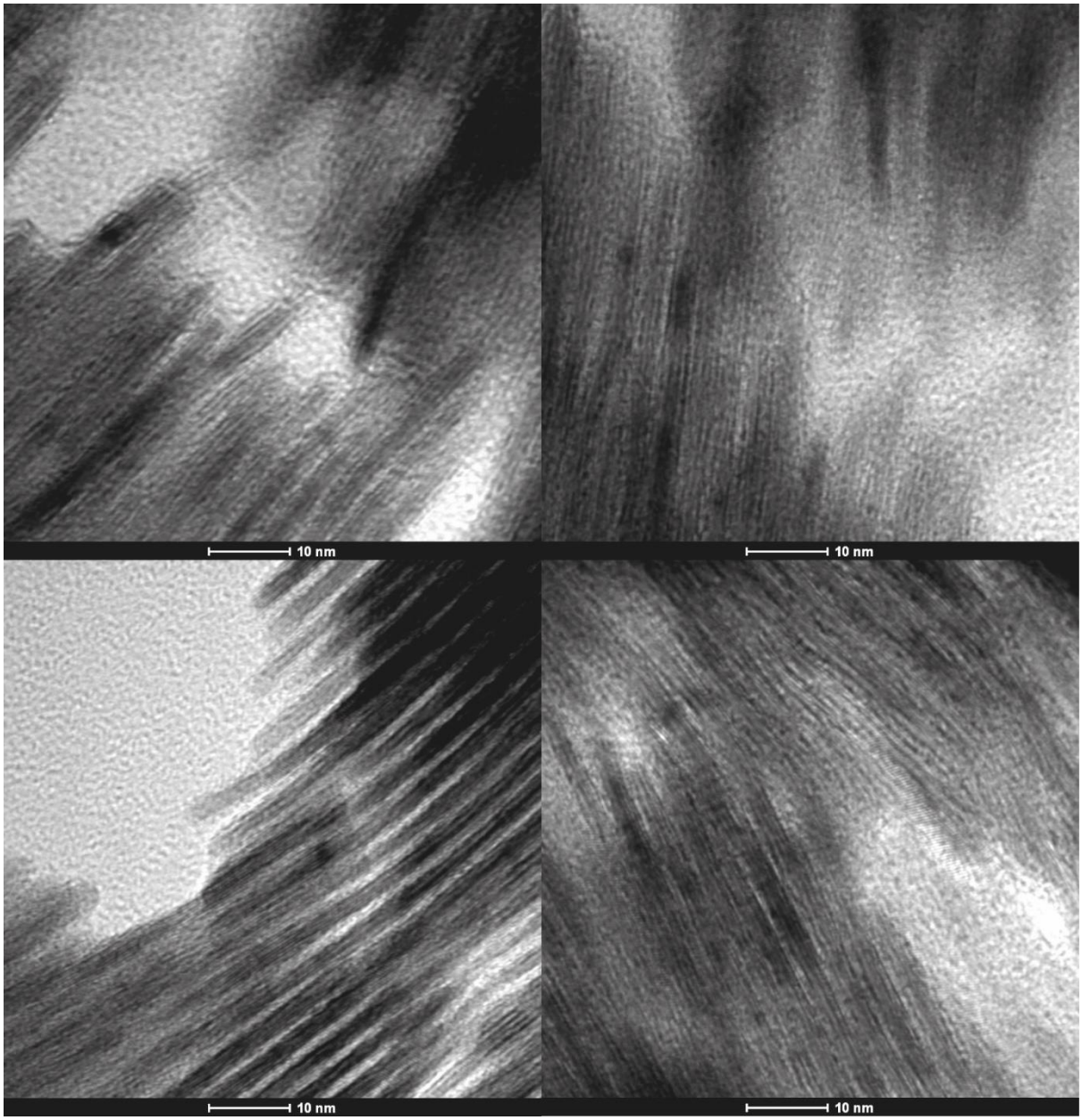

Figure S6. High-resolution TEM images of stacked $Cu_{2-x}Se$ NSs. The atomic layers (~4 per NSs) can be distinguished.

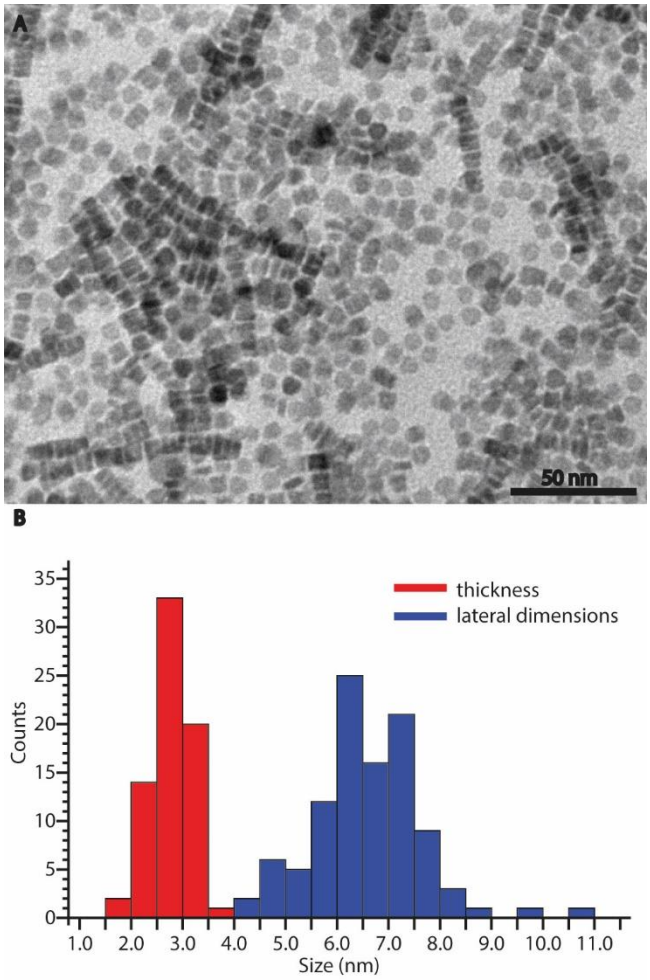

Figure S7. **A.** TEM image of control experiment without halides, using only Cu(I) acetate as precursor. **B**. Histogram of thickness and lateral dimensions of the NCs shown in A, showing a low aspect ratio.

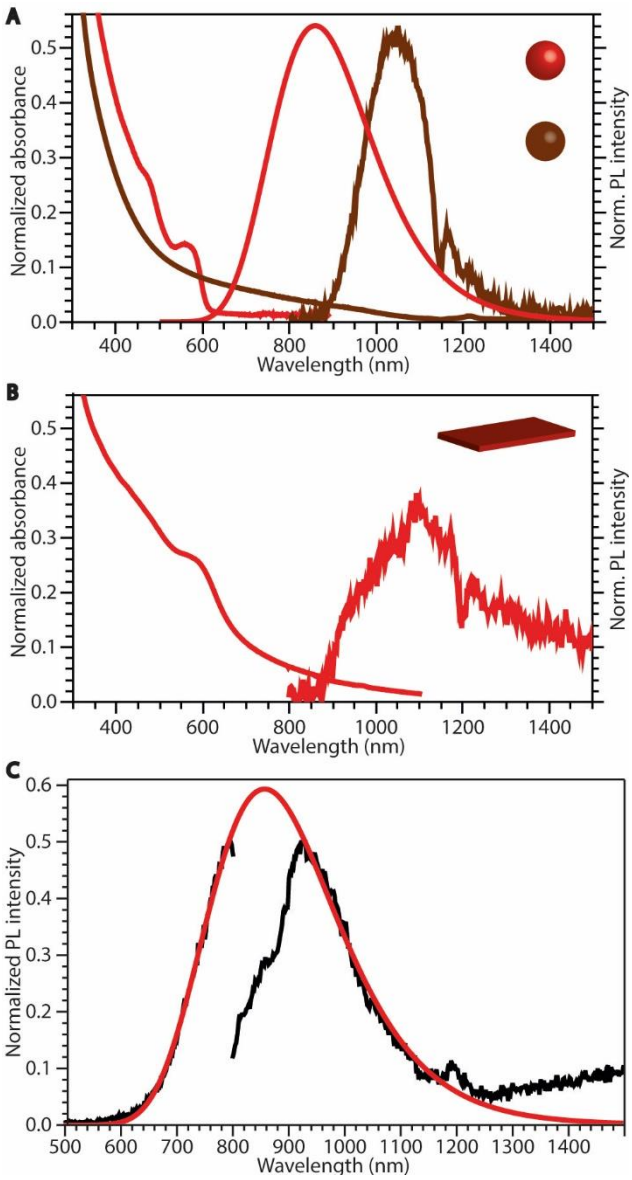

Figure S8. A. Absorption and PL spectra of CdSe and $CuInSe_2$ quantum dots. The dips in the PL spectrum of the $CuInSe_2$ NCs at ~1100 nm are due to absorption by toluene. The PL spectrum of the CdSe quantum dots (red line) is a two-sided Gaussian fit combining PL spectra measured with two different sets of gratings and detectors (the measured spectra are shown in C.) **B.** Absorption and PL spectra of ultrathin CdSe nanosheets. The absorption by toluene is clearly observed at ~1100 nm. **C.** Normalized PL signals as measured on two different detectors (black) and the two-sided Gaussian fit through both measured curves (red). For the measurements a Hamamatsu R928 detector with a monochromator grated at 500 nm, and a Hamamatsu R5509-72 PMT with a monochromator grated at 1200 nm were used.

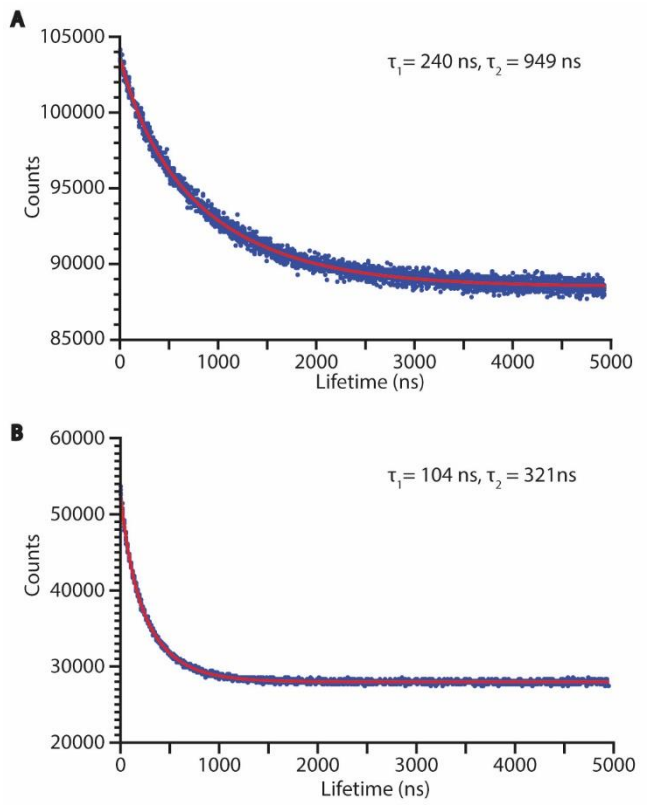

Figure S9. **A.** PL decay curve of product Cu^{+}-doped CdSe quantum dots obtained by Cu^{+} for Cd^{2+} cation exchange in template $Cu_{2-x}Se$ NCs. **B.** PL decay curve of product $CuInSe_2$ quantum dots obtained by partial Cu^{+} for In^{3+} cation exchange in template $Cu_{2-x}Se$ NCs. Both decay curves were fitted with a two-exponential function (red line). The decay times are indicated in the figure.

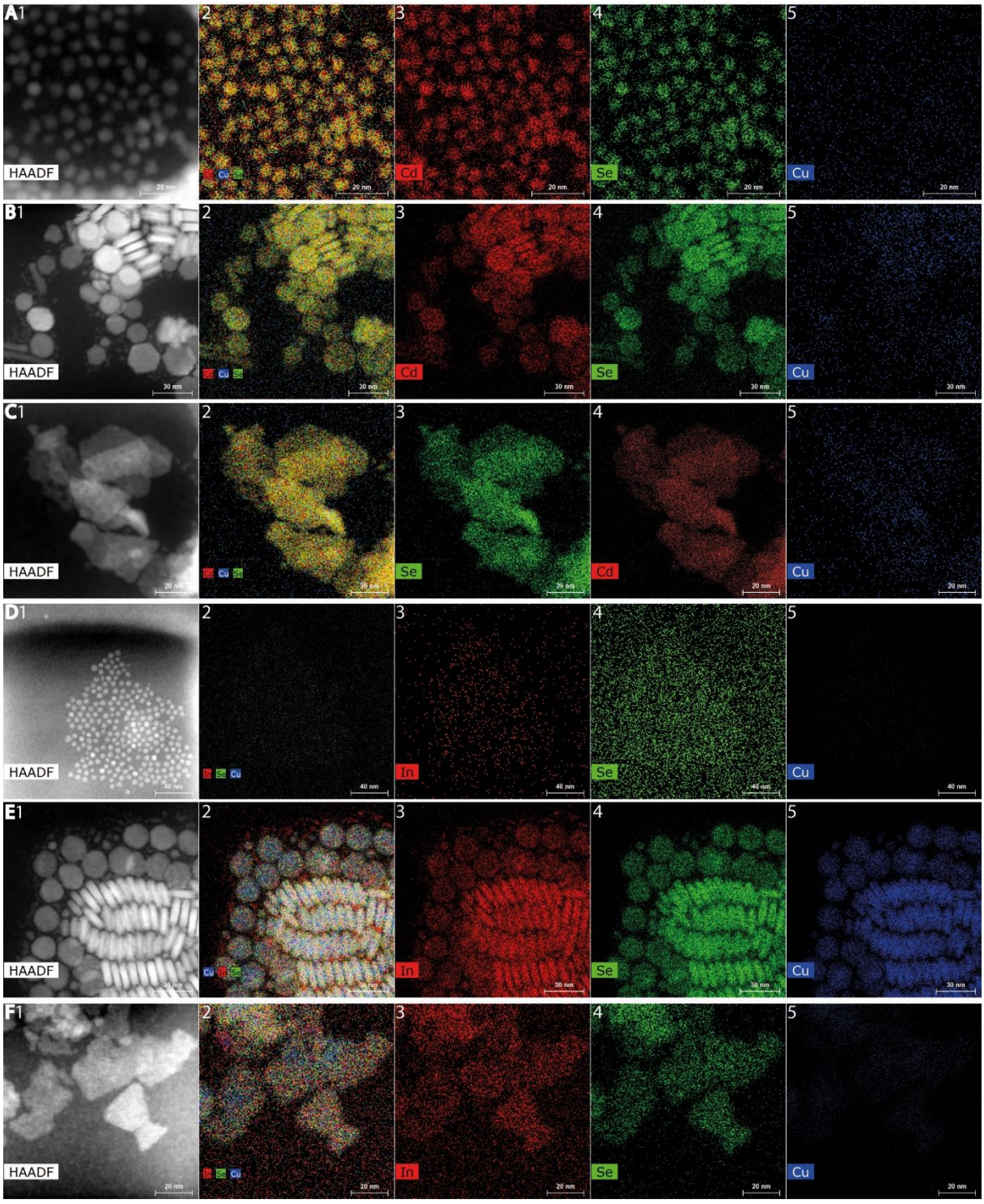

Figure S10. HAADF-STEM Elemental maps. **A-C.** CdSe nanocrystals: dots (A), platelets (B) and nanosheets (C). **D-F.** $CuInSe_2$ nanocrystals: dots (D), platelets (E), nanosheets (F). The maps confirm the successful cation exchange for both compositions and show qualitatively the same results as the bulk EDS measurements discussed in the main text.

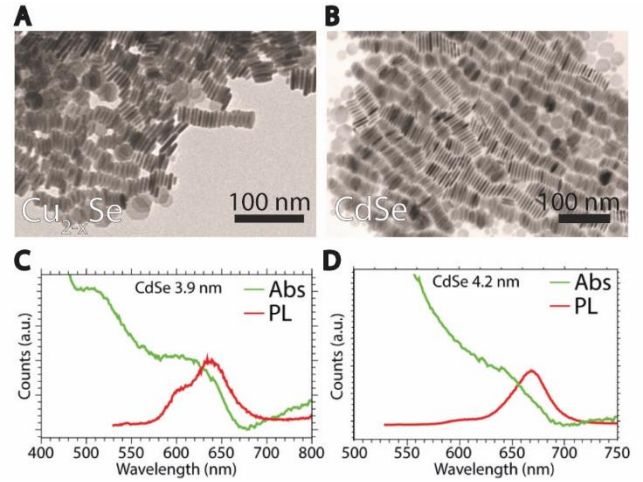

Figure S11. A TEM image of template $Cu_{2-x}Se$ nanoplatelets with a thickness of 4.2 nm. **B.** TEM image of product CdSe nanoplatelets obtained by Cu^{+} for Cd^{2+} cation exchange using the $Cu_{2-x}Se$ NCs displayed in A as templates. **C.** Absorption and PL spectra of 3.9 nm thick product CdSe nanoplatelets obtained by Cu^{+} for Cd^{2+} cation exchange in template $Cu_{2-x}Se$ nanoplatelets. **D.** Absorption and PL spectra of 4.2 nm thick product CdSe nanoplatelets obtained by Cu^{+} for Cd^{2+} cation exchange in template $Cu_{2-x}Se$ nanoplatelets.

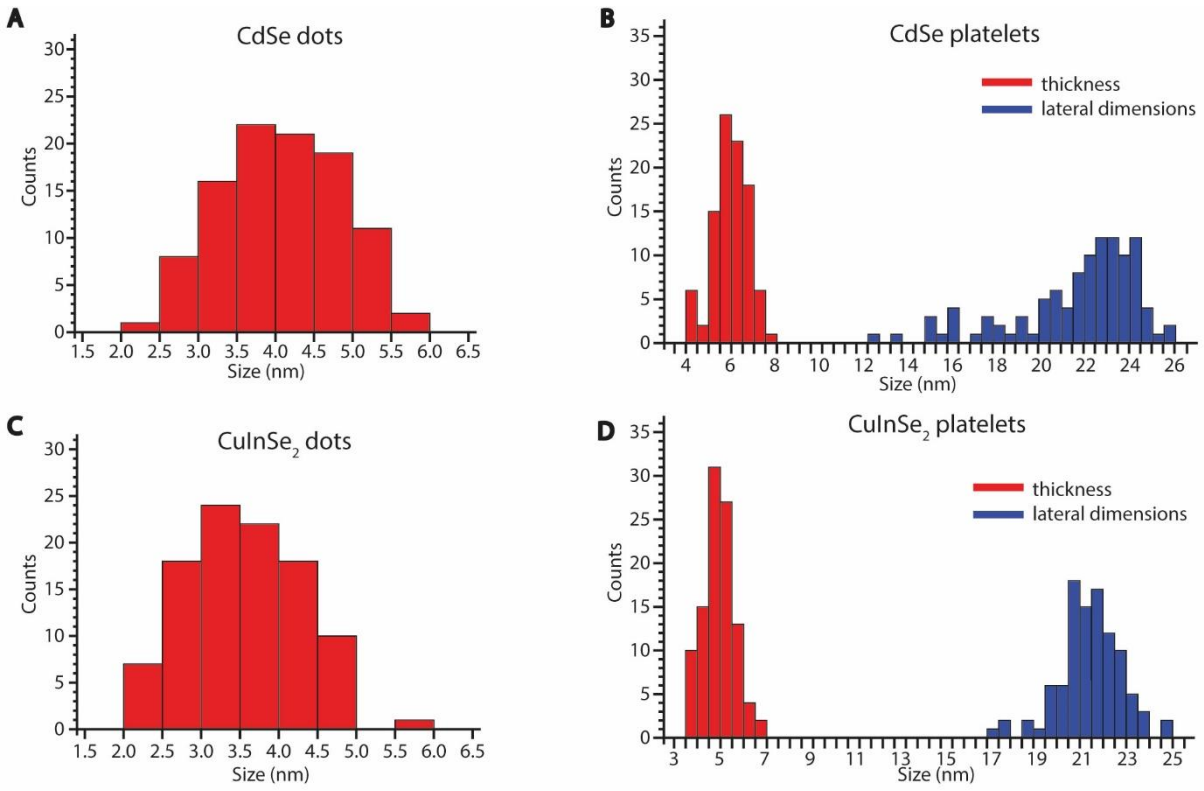

Figure S12. Size histograms of NCs shown in Figure 4 in the main text.

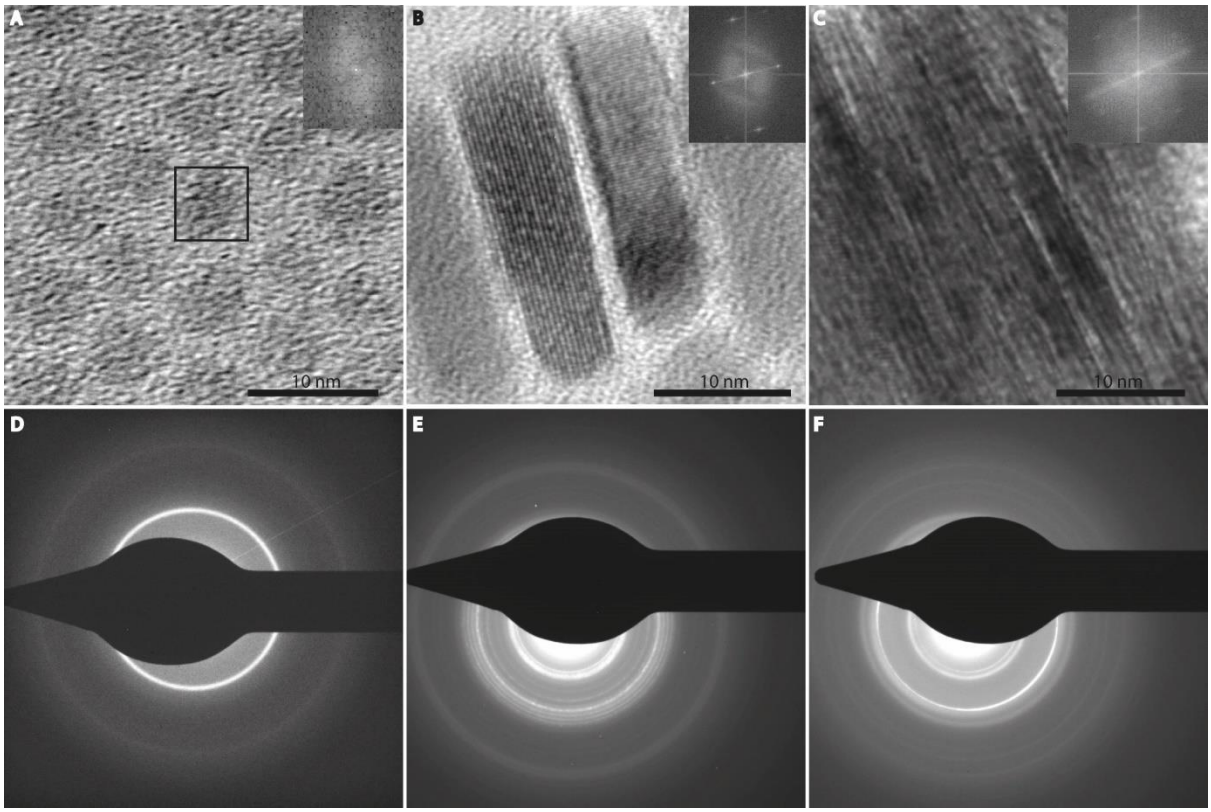

Figure S13. **A-C**. High-resolution TEM images of $Cu_{2-x}Se$ quantum dots (A), nanoplatelets (B) and nanosheets (C). The inset in A shows the FFT of the NC in the frame, the insets in B and C show the FFT of the full images. The scale bars correspond to 10 nm. **D-F**. Electron diffraction ring patterns of quantum dots (D), nanoplatelets (E) and nanosheets (F).

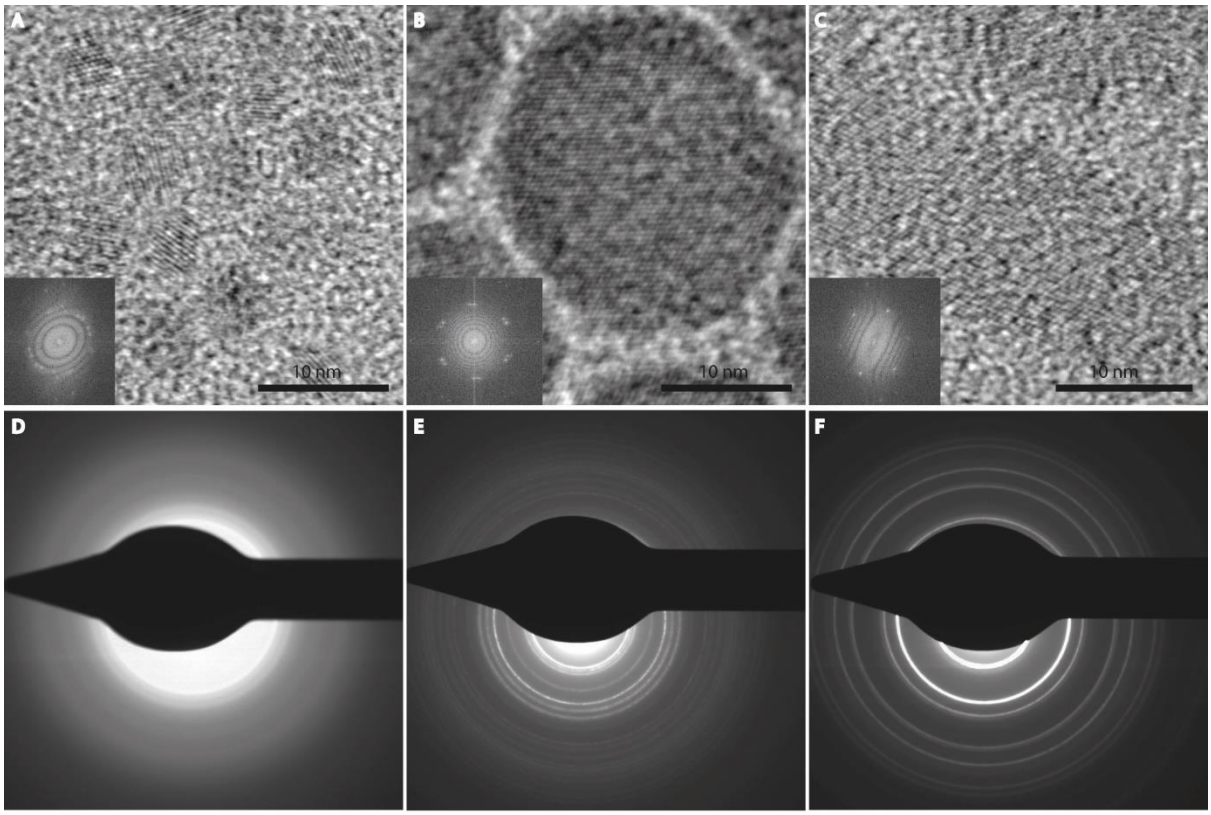

Figure S14. **A-C**. High-resolution TEM images of CdSe quantum dots (A), nanoplatelets (B) and nanosheets (C). The insets show the FFT of the images. The scale bars correspond to 10 nm. **D-F**. Electron diffraction ring patterns of quantum dots (D), nanoplatelets (E) and nanosheets (F).

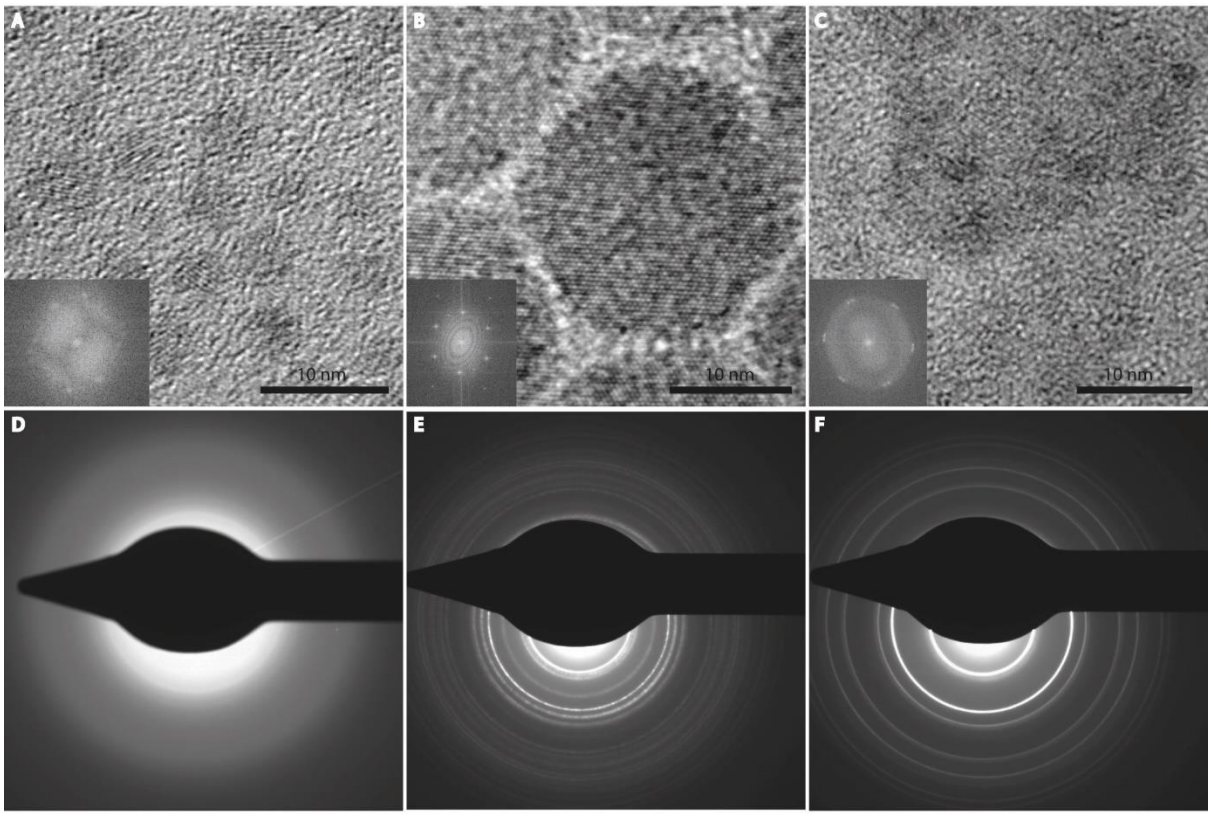

Figure S15. **A-C**. High-resolution TEM images of $CuInSe_2$ quantum dots (A), nanoplatelets (B) and nanosheets (C). The insets show the FFT of the images. The scale bars correspond to 10 nm. **D-F**. Electron diffraction ring patterns of quantum dots (D), nanoplatelets (E) and nanosheets (F).

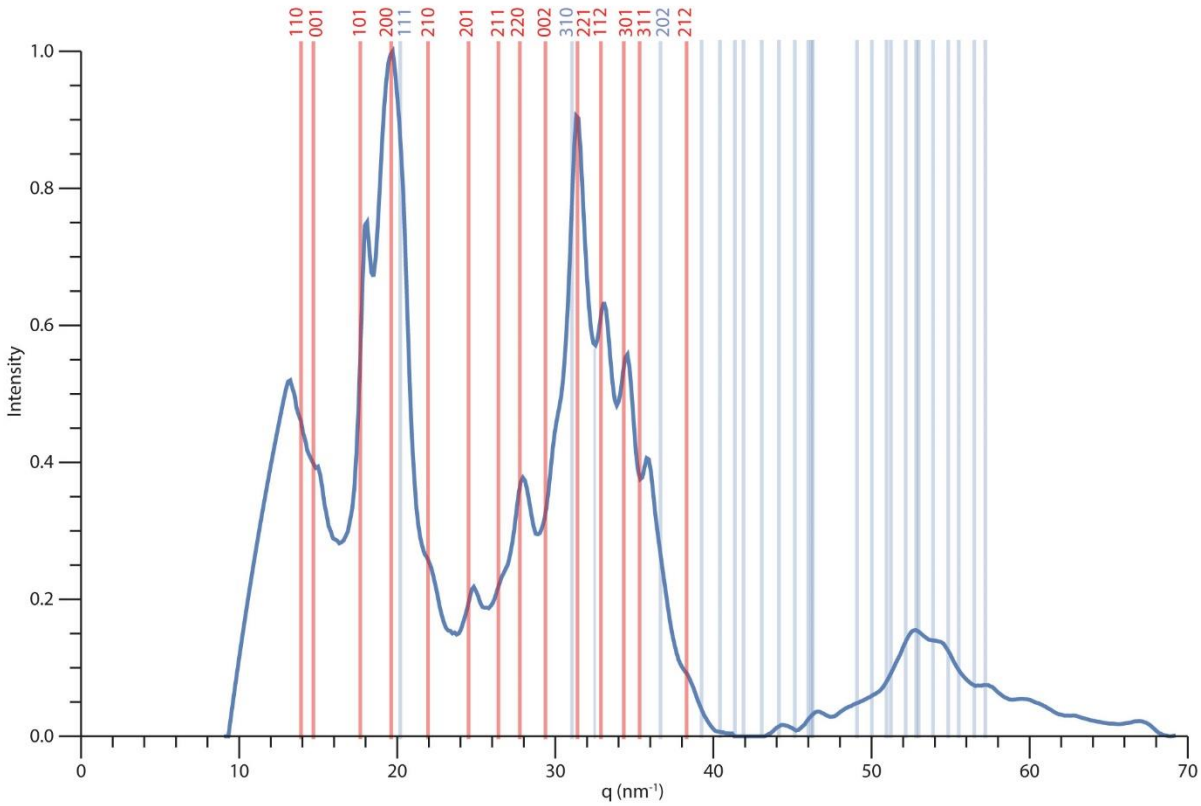

Figure S16. Integrated ED pattern of $Cu_{2-x}Se$ nanoplatelets, with the bulk XRD reference pattern for umangite as vertical lines. The red lines indicate the good matches (at low q values). The corresponding lattice planes are indicated.

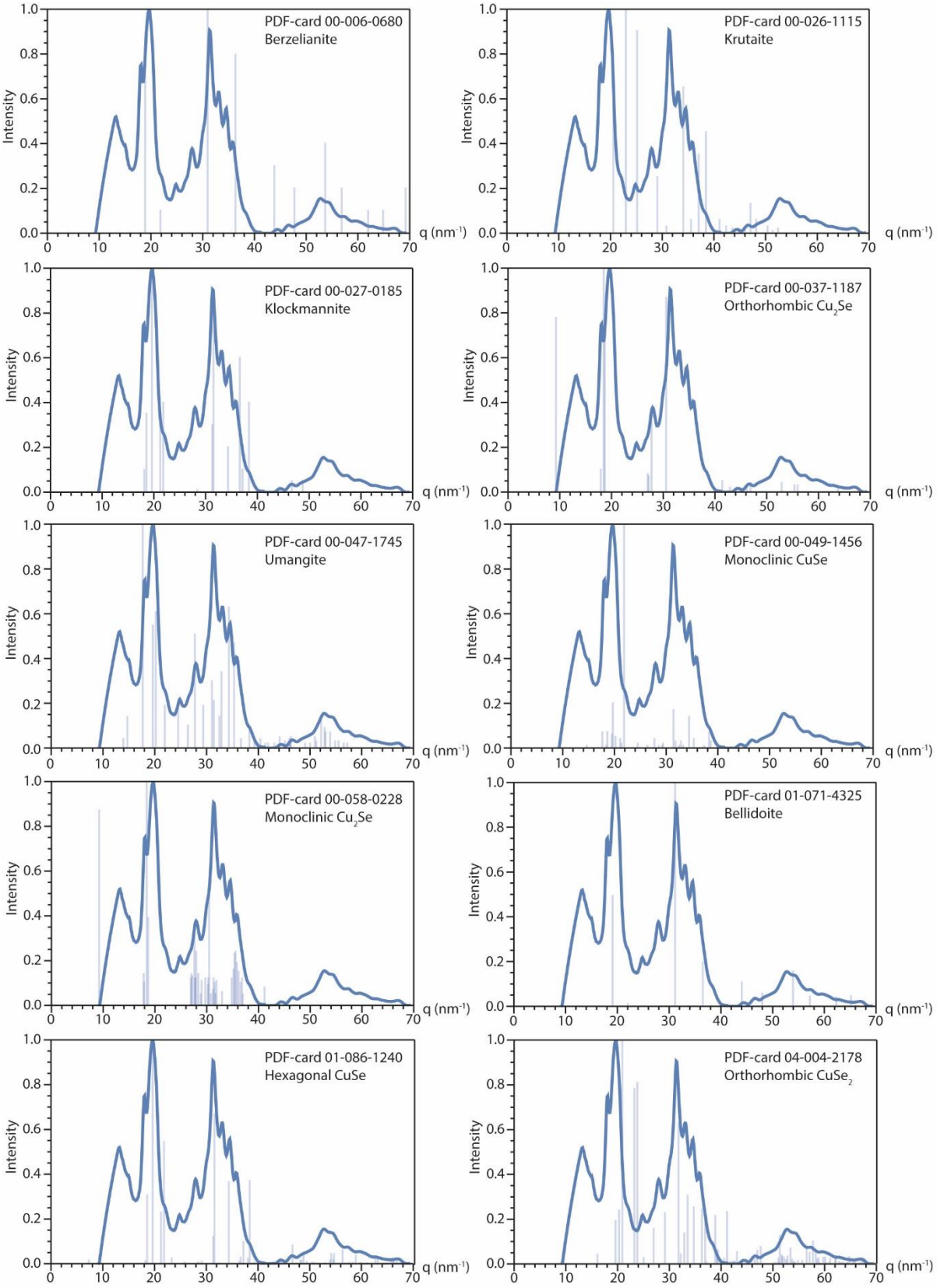

Figure S17. Integrated ED pattern of $Cu_{2-x}Se$ nanoplatelets plotted with different bulk XRD references. The Umangite reference fits best to the signal.

References

1. Merijanian, A.; Zingaro, R. A.; Sagan, L. S.; Irgolic, K. J. The 1H(Se-H) NMR Chemical Shift in Selenols and the Fundamental Se-H Stretching Frequency. *Spectrochim. Acta Part A Mol. Spectrosc.* **1969**, *25*, 1160–1165.

2. Yagüe, J. L.; Agulló, N.; Fonder, G.; Delhalle, J.; Mekhalif, Z.; Borrós, S. Thiol versus Selenol SAMs as Nucleation Enhancers and Adhesion Promoters for Plasma Polymerized Pyrrole on Copper Substrates. *Plasma Process. Polym*. **2010**, *7*, 601-609.

3. Ford, P. C.; Cariati, E.; Bourassa, J. Photoluminescence Properties of Multinuclear Copper(I) Compounds. *Chem. Rev.* **1999**, *99*, 3625-3647.

4. Shriver & Atkins – Inorganic Chemistry, 5th Ed., 2010, Oxford Pub.